Hot deformation behavior of in situ synthesized Ti composite reinforced with 5 vol.% (TiB + TiC) particles

Feng-cang Ma · Wei-jie Lu · Ji-ning Qin ·
Di Zhang

Abstract In this paper, 5 vol.% (TiB + TiC)/Ti-1100 composite was fabricated using in situ techniques. Hot-deformation behavior of the composite was studied by hot compression tests in the temperature range 1,000–1,150 °C under different strain rates. It was found that solid solute C element in Ti matrix has obvious effect on the hot-deformation behavior of the composite by increasing the $(\alpha + \beta)/\beta$ transus temperature. Variation in the volume ratio of α/β phase and the effect of reinforcements result in a change in hot-deformation behavior of the composite. The effect of reinforcements on hot deformation behavior of the composite is more obvious in the $(\alpha + \beta)$ phase field than in the β phase field.

Introduction

Titanium alloys find application in a wide variety of technological fields including aerospace, marine, chemical, sporting goods, power generation and biomedical. This is attributed to the higher specific strength, specific modulus and elevated-temperature properties that some of these alloys offer. These properties are expected to further improve by incorporating low density, high modulus, and high strength ceramic reinforcements into the titanium

F.-c. Ma
Henan University of Science and Technology, Luoyang 471039, P.R. China

F.-c. Ma · W.-j. Lu · J.-n. Qin · D. Zhang (✉)
State Key Laboratory of Metal Matrix Composites, Shanghai Jiao Tong University, Shanghai 200030, P.R. China
e-mail: zhangdi@sjtu.edu.cn

matrix. Most of the research work so far is concentrated on continuous fiber reinforced titanium matrix composites [1, 2]. However, these composites are highly anisotropic in properties, and their fabrication is complex and expensive. Interest has increased in ceramic particulate reinforced titanium matrix composites in recent years, because these composites have isotropic characteristics and can be processed inexpensively by using conventional technologies, such as ingot metallurgy (IM), casting and powder metallurgy (PM). Among the ceramic particulates, TiC and TiB are particularly attractive since they are completely compatible with titanium matrix [3–7]. Recently, TMCs with better properties can be prepared by the in situ technique, which overcomes the shortcomings of traditional techniques, such as the problems of pollution of reinforcements and wettability between ceramic particles and matrix encountered in the casting technique. Therefore in situ synthesized TMCs have been widely studied [8–10]. In a previous work, Zhang et al [11] prepared (TiB + TiC)/Ti composites utilizing the chemical reaction between Ti and B_4C powder as following reaction:

$$Ti + B_4C \rightarrow 4TiB + TiC. \qquad (1)$$

However, the machining property of these composites is inferior because of the distribution of the reinforcement with high hardness in the soft matrix. It is difficult to machine a work-piece with complex configuration, which restricts the application and development of the composites. In order to solve these problems, hot deformation or superplastic deformation of materials can be used, which saves raw materials and reduces cost. Studies on hot deformation of titanium matrix composites have been carried out all over the world in recent years. Reports on the high temperature deformation of TiC particle-reinforced titanium matrix

composites have dealt with the superplasticity phenomenon [12]. Recently, Wang et al. [13] studied the superplastic deformation of 1 vol.% (TiB + TiC)/Ti composites, they found that the activation energies of this material are 641 kJ mol^{-1} at 1,000 °C but only 275 kJ mol^{-1} at 1,020–1,080 °C. And they thought that the different activation energies were resulted from different deformation mechanisms in this temperature range. The aim of this research is to reveal the deformation behavior of 5 vol.% (TiB + TiC)/Ti composites in the temperature range 1,000–1,150 °C under different strain rates.

Experimental procedure

The material used in this experiment was a Ti-1100 alloy reinforced with (TiB + TiC) (5 vol.%) ceramic particle. For preparing (TiB + TiC)/Ti-1100 TMCs, the raw materials were grade I sponge titanium, B$_4$C powder (99.8%, average particle size, 5–7 μm), aluminum thread (98%), crystal silicon (99.5%), sponge zirconium (98.8%) and master alloys of other alloying elements such as Ti–Sn, Al–Mo. The nominal alloy composition of Ti-1100 was Ti–6Al–2.75Sn–4Zr–0.4Mo–0.45Si. The composite was prepared in a consumable vacuum arc remelting furnace (VAR) utilized the reaction between Ti and B$_4$C powder as formula (1). In order to ensure the chemical homogeneity of the composite, the ingots were melted at least three times. After casting, the alloying element contents were measured by chemical method, and the results were presented in Table 1. The ingots breakdown was performed at 1,150 °C and cooled in air. Phase identification was carried out via X-ray diffraction using D-max IVA automatic X-ray diffractometer. Hot compression specimens were cut from the ingots after breakdown. The hot compression specimens were a column 8 mm in diameter and 12 mm in length. Hot compression tests were conducted using a Gleeble-1500 thermo-simulation test machine. The compression tests were conducted along the direction in the length of the column, and the compression ratio was 0.5 ($l_0 - l$/l_0, where l_0 and l was the length along the compress direction before and after compress, respectively). The specimens after compression were quenched into water. No crack was found on the specimens' surface by eyes after compression. Samples for optical microscopy (OM) were cut from the specimens after compression. Then the samples were prepared using conventional techniques of grinding and mechanical polishing. The samples were etched in Kroll's reagent (composition: 1–3 mL HF, 2–6 mL HNO$_3$, 100 mL water). A LECO 2000 image analyzer was used to characterize the microstructures of the samples, and it was also used to measure the volume of the α phase in the composite utilizing specific software by metallographic method.

Results and discussion

Phase identification

Figure 1 shows XRD patterns of the specimen. It indicates that TiB has formed in the composite. The result of the XRD analysis confirms that B$_4$C powder has reacted with titanium matrix. The distribution of TiB and TiC particles in the composite is shown in Fig. 2. It can be seen that reinforcements are distributed uniformly in the titanium matrix. The results of energy dispersion X-ray spectrometer (EDS) [14, 15] show that the needle-shaped reinforcements are TiB, while the equiaxed-shaped reinforcements are TiC. The difference in shape of TiB and TiC reinforcements results from their solidification paths and crystal structure during casting process.

The β transus temperature of in situ (TiB + TiC)/Ti-1100 composites

Hot deformation behavior of Ti alloys and its composites is quite different when the deformation is performed whether in the (α + β) phase field or in the β field. So the (α + β)/β transus temperature is a very important parameter for the hot deformation study of Ti alloys and its composites. Metallographic techniques were used to measure the β transus temperature of the composite. The results are presented in Fig. 3. From Fig. 3, the β transus temperature of the present composite was identified as 1,115 °C. There is an about 100 °C increase in β$_t$ compared to Ti-1100 (β$_t$ temperature is about 1,015 °C [16]). From the Ti–B binary alloy phase diagram, it can be known that B elements are almost immiscible in α-Ti, and the effect of B element is not obvious on β$_t$ of matrix. In another work by these authors, it was found that solute C element in Ti matrix increase the β$_t$ of the matrix alloy obviously [17]. For the present composite, the increase in the β$_t$ of the matrix results from the solute C element in Ti matrix.

To interpret the effect of C on β$_t$ of the composite, it is helpful to examine the Ti–Al–C ternary phase diagram. The present matrix alloys contain α stabilizers Al, Sn, Zr, and O, the effect of which can be represented in terms of an Al equivalent content. According to Rosenberg [18], the equivalent of Al content can be expressed as

Table 1 Contents of alloying elements in the composite (as cast)

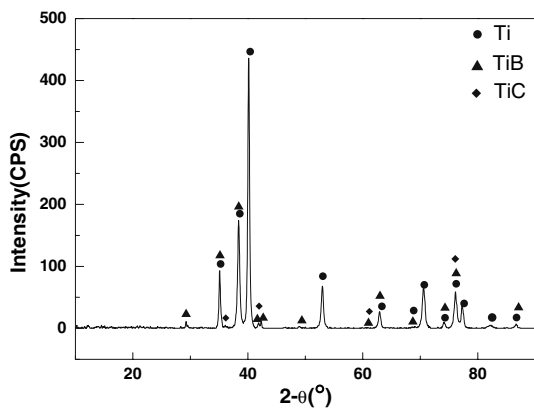| Element	Al	Sn	Zr	Mo	Si	O
Content (mass%)	6.13	2.72	4.02	0.41	0.46	0.08

Fig. 1 X-ray diffraction patterns of 5 vol.% (TiB + TiC)/Ti-1100 composite
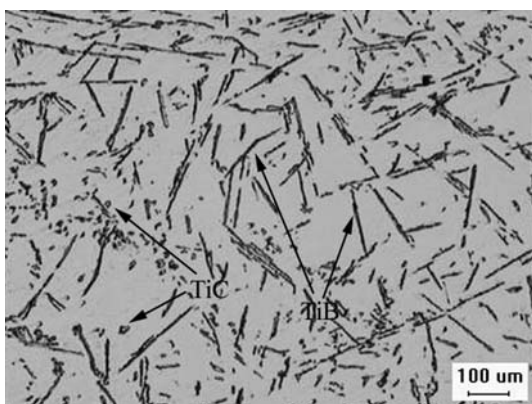

Fig. 2 The distribution of reinforcements in 5 vol.% (TiB + TiC)/Ti-1100 composite (unetched)

$[Al]_{eq} = [Al] + [sn]/3 + [Zr]/6 + 10[O]$. From Table 1, for the present matrix alloy $[Al]_{eq}$ is calculated to be 8.35. Thus we can refer to the Ti–8Al–C phase system to discuss the $(\alpha + \beta)/\beta$ transus temperature of the matrix alloy under study. A vertical section of the Ti–8Al–C alloy phase diagram [19] is shown in Fig. 4, and the present composition of the composite is marked with A in Fig. 4. According to this vertical section, the addition of carbon increase the $(\alpha + \beta)/\beta$ transus temperature rapidly when the
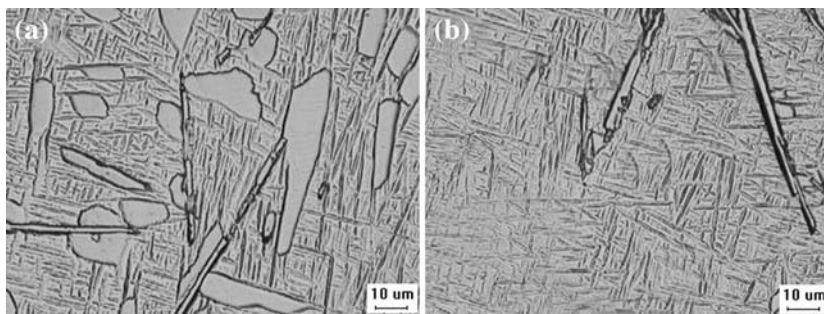
C concentration in matrix alloy is below 0.28 wt.%, and the β transus temperature of the composite identified in this experiment is lower slightly than that presented in the Ti–8Al–C ternary phase diagram, which maybe results from Mo and Si in matrix which are β stabilizers.

From the results about the β_t of the composite, it can be know that the reaction in formula (1) cannot perform completely, and some C element dissolve in Ti matrix during the preparation process of in situ (TiB + TiC)/Ti-1100 composite. Solid solute C element in Ti matrix increases the β_t of the composite obviously.

Hot deformation behavior of the 5 vol.% (TiB + TiC)/Ti-1100 composite

Optical micrographs of the composite after hot compression are presented in Fig. 5. The stress–strain curves of the hot compression tested the composite are presented in Fig. 6. It is apparent that all the stress–strain flow curves show an initial work hardening period followed by a regime of near steady-state flow. Higher peak stresses are observed at higher strain rates and lower temperatures. In entire temperature range (1,000–1,150 °C), flow stresses exhibit a long steady state regime after decreased from the peak stresses, which results from hardening and softening of the composite. Generation and pile-up of dislocations result in the work hardening at the primary stage of deformation. Subsequently, the rate of hardening by generation of dislocations is balanced by the rate of softening due to dislocations annihilation, thus resulting in the constant flow stress deformation.

The power–Arrhenius relationship [20] is used to calculate the activation energies for plastic deformation and strain rate sensitivity index

$$\dot{\varepsilon} = A \cdot \sigma^n \cdot \exp\left(-\frac{Q}{RT}\right) \qquad (2)$$

in above formula, $\dot{\varepsilon}$, A, σ, n, Q, R and T are strain rate, a constant of the material, stress, stress index, activation energies for plastic deformation, gas constant and absolute temperature, respectively. From formula (2), the following
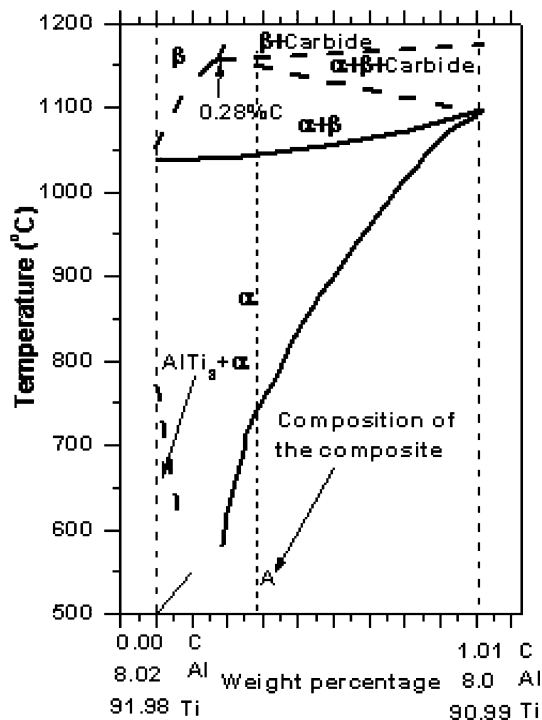
Fig. 3 Optical micrographs of the composite after quenched: (a) 1,110 °C, (b) 1,120 °C

Fig. 4 Vertical section of Ti–8Al–C equilibrium alloy phase diagram

equation can be obtained ($m = 1/n$, m, strain rate sensitivity index):

$$m = \frac{\partial \lg \sigma}{\partial \lg \dot{\varepsilon}} \tag{3}$$

$$Q = \frac{1}{m} \cdot R \cdot \frac{\partial \lg \sigma}{\partial (1/T)} \tag{4}$$

log σ vs. log $\dot{\varepsilon}$ plot is presented in Fig. 7. From Fig. 7, it can be found that the value of m is not a constant in the entire temperature range, and it increase with the increasing of test temperature. The activation energies were calculated with the slopes of log σ vs. (2,000/T) curves (Fig. 8) and the values of m. The activation energies for

plastic deformation under 10^{-2}, 10^{-1} and 10^{0} s^{-1} at 1,000, 1,050, 1,100 and 1,150 °C are calculated to be 513.1, 310.7, 260.6, 251.5 kJ/mol, respectively (with average slope = 4.04). The great difference in the activation energy is indicative of change in deformation behavior. The deformation behavior of the composite in this temperature range may be analyzed by two factors. One is the deformation of α phase and β phase, and the other is the effect of reinforcement particles on the deformation of the α phase and the β phase.

The effect of variation in α/β phase ratio on the hot behavior of the composite

From Fig. 4 and the results about β_t of the composite, it can be known that the composite is in the ($\alpha + \beta$) phase field in the temperature range from 1,000–1,100 °C. When the deformation was performed in the ($\alpha + \beta$) phase field, α phase and β phase deform simultaneously. In order to analyze the resultant deformation of the α phase and the β phase, an iso-strain rate model [21] was put forward. In the iso-strain rate mode, where there is a stress distribution between the α phase and the β phase such that the resultant matrix deformation rates (or the accommodation rates) in the two phases are equal, and the model is depicted by the following formula:

$$\dot{\varepsilon}_{\text{total}} = \dot{\varepsilon}_\alpha = \dot{\varepsilon}_\beta \tag{5}$$

$$\sigma_{\text{total}} = f_v^\alpha \sigma_\alpha + f_v^\beta \sigma_\beta \tag{6}$$

in above formula, $\dot{\varepsilon}_{\text{total}}$, $\dot{\varepsilon}_\alpha$, $\dot{\varepsilon}_\beta$, σ_{total}, f_v^α, f_v^β, σ_α and σ_β are the resultant matrix deformation rates, α phase strain rate, β phase strain rate, applied total stress, volume fraction of the α phase, volume fraction of the β phase, the stress undertaken by the α phase and the stress undertaken by the β phase, respectively. Due to the β phase considerably lower flow stress than the α phase [16], the deformation of the β phase is constrained by the α phase consequently, and the resultant matrix deformation is mainly controlled by the α phase. The activation energies for plastic deformation of the composite as a function of the volume of the α phase

Fig. 5 Optical micrographs of the composite after hot deformation (**a**) 1,100 °C, (**b**) 1,150 °C under 10^{-1} s^{-1} strain rate (The compression direction during hot deformation as marked on the Figs)
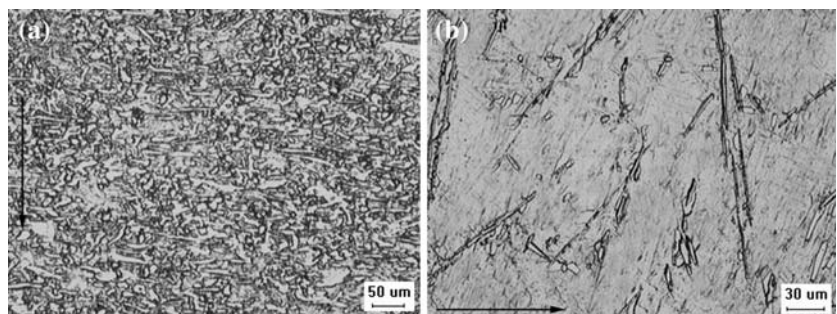
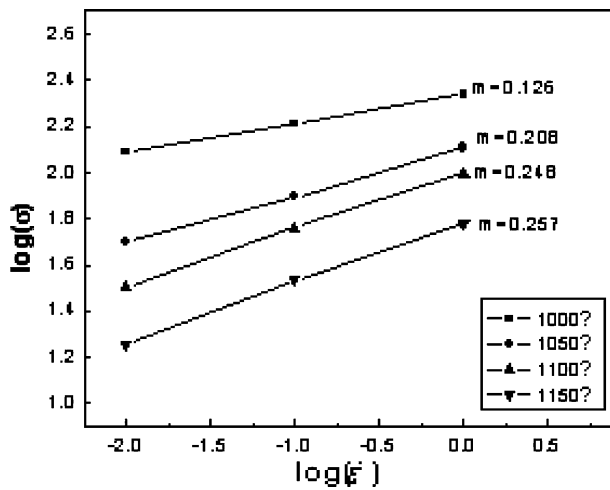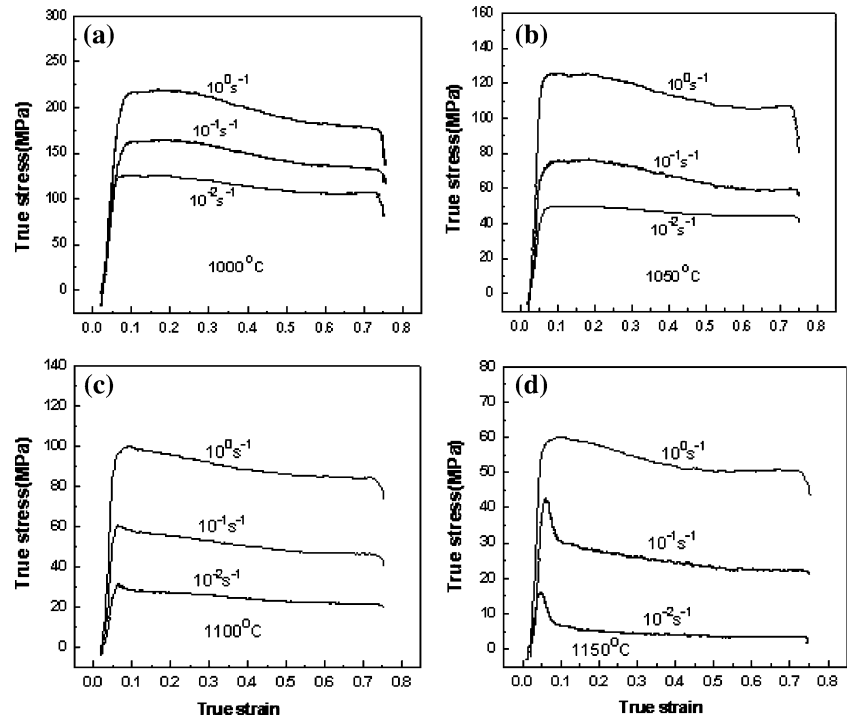**Fig. 6** The stress–strain curves for 5 vol.% (TiB + TiC)/Ti-1100 composite during hot compression

Fig. 7 log σ vs. log ($\dot{\varepsilon}$) curves at 1,000, 1,050, 1,100 and 1,150 °C under 10^{-2}, 10^{-1} and 10^0 s^{-1} strain rate, respectively
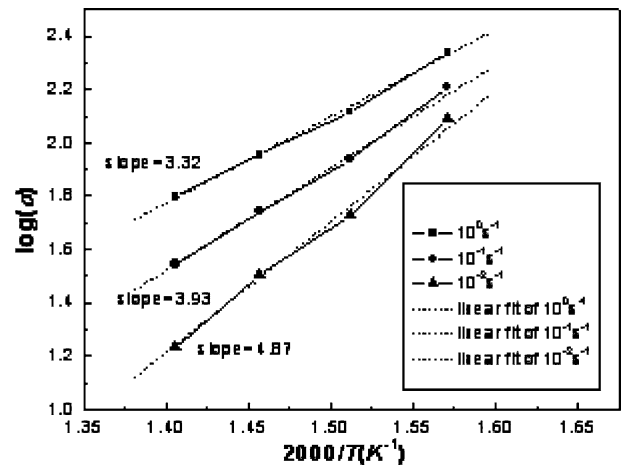
Fig. 8 log σ vs. (2000/T) curves for 5 vol.% (TiB + TiC)/Ti-1100 MMC

are presented in Fig. 9, and it can be found that the plastic deformation activation energies of the composite increase accordingly with the increasing of the volume fraction of the α phase. These discusses are consistent with activation energies of near α monolithic Ti alloys reported by other researchers, such as: IMI834 and CP-2, activation energy for plastic deformation in the ($\alpha + \beta$) phase field are 310 and 346 kJ/mol, but the values of that in the β phase field range from 180 to 220 kJ/mol [16].

The activation energy for plastic deformation of the composite at 1,150 °C (251.5 kJ/mol) is lager slightly than

that of monolithic Ti alloys in the β phase field. This result indicates that the deformation mechanism of the composite is controlled by the β phase in the β phase field.

The effect of reinforcements on the hot behavior of the composite

From above results, it can be seen that the activation energies of the composite are higher than that of monolithic Ti alloys in all phase fields, and the difference between them are very large in the ($\alpha + \beta$) phase field (the values
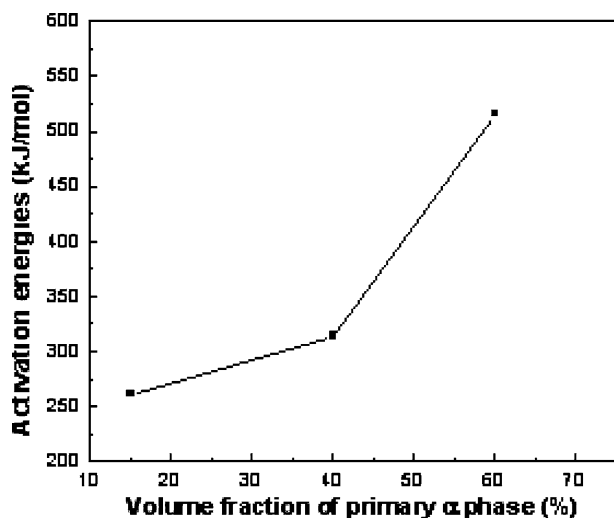
Fig. 9 The activation energy as a function of volume fraction of primary α phase in the composite

are 513.1 and 310 kJ/mol, respectively), which is the effect of reinforcements. The effect of reinforcement particles on matrix deformation will be discussed in the β phase field and in the $(\alpha + \beta)$ phase field, respectively.

When the deformation is performed in the $(\alpha + \beta)$ phase field, especially at a lower temperature, the deformation of the composite is controlled by α phase. Because α titanium deform by slip on basal and prismatic planes [22], reinforcements may impede the movement of dislocations in the α phase effectively, which result in higher activation energy for plastic deformation. But the activation energy for plastic deformation of the composite in the β phase field (251.5 kJ/mol) is lager slightly than that of monolithic Ti alloys in the β phase field (180–220 kJ/mol), which indicates that reinforcements do not affect the hot deformation behavior of the composite so obviously as in the $(\alpha + \beta)$ phase field. In general, the effect of reinforcement on the hot deformation behavior of the composite is different in different temperature ranges. The effect is more obvious in the $(\alpha + \beta)$ phase field than in the β phase field.

Conclusions

Utilizing the reaction between B_4C powder and Ti to prepare in situ (TiB + TiC)/Ti composite, the reaction cannot perform completely, and some C element dissolve in Ti matrix during preparation process. Solid solute C element in matrix increases the β_t of the matrix about 100 °C for the

5 vol.% (TiB + TiC)/Ti-1100 composite. Hot deformation behavior of the composite change greatly in the temperature range from 1,000 to 1,150 °C, and activation energy for plastic deformation decrease rapidly with the increasing of temperature. The change results from the variation in α/β phase ratio and the effect of reinforcements. Reinforcements incorporation results in higher activation energies for plastic deformation, and its effect is more obvious in the $(\alpha + \beta)$ phase field than in the β phase field.

References

1. Baumann F, Brindly PK, Smish SD (1990) Metall Trans A 21(6):1559
2. Chiang KT, Loh DH, Liaw PK, Diaz ES (1995) Metall Trans A 26(12):3249
3. Ranganath S, Roy T, Mishra RS (1996) Mater Sci Technol 12(3):219
4. Ranganath S (1997) J Mater Sci 32(1):1
5. Soboyejo WO, Lederich RJ, Sastry SML (1994) Acta Metall Mater 42(8):2579
6. Ma ZY, Tjong SC, Geng L (2000) Scripta Mater 42(4):367
7. Tjong SC, Ma ZY (2000) Mater Sci Eng R 29(3):49
8. Lu WJ, Zhang XN, Zhang D, Wu RJ, Sakata T, Mori H (2001) Scripta Mater 44(10):2449
9. Tsang HT, Chao CG, Ma CY (1996) Scripta Mater 35(8):1007
10. Man HC, Zhang S, Cheng FT, Yue TM (2001) Scripta Mater 44(12):2801
11. Zhang XN, Lu WJ, Zhang D, Wu RJ (1999) Scripta Mater 41(1):39
12. Kobayashi M, Ochiai S, Funami K, Ouchi C, Suzuki S (1994) Mater Sci Forum 170–172:549
13. Wang MM, Lu WJ, Qin JN (2005) Scripta Mater 53(2):265
14. Lu WJ, Zhang D, Zhang XN, Wu RJ (2001) J Alloys Comp 327:240
15. Lu WJ, Zhang D, Zhang XN, Wu RJ (2001) J Alloys Comp 327:248
16. Weiss I, Semiatin SL (1999) Mater Sci Eng A 263(2):243
17. Ma FC, Lu WJ, Qin JN, Zhang D (2006) Mater Lett 60(3):400
18. Rosenberg HW (1970) In: Jaffee RI, Promisel NE (eds) The science, technology and application of titanium. Pergamon, New York, p 851
19. Villars P, Prince A, Okamoto H (1997) Handbook of ternary phase diagrams, vol. 2. ASM International, Materials Park, OH, p 2906
20. Whittenberger JD (1986) Mater Sci Eng A 77(1):103
21. Wert JA, Paton NE (1983) Metall Trans A 14(12):2535
22. Krishna VG, Prasad YVRK, Birla NC, Rao GS (1997) J Mater Process Technol 71(3):377